

**NISTIR 6448**

---

---

Comparison of Algorithms to Calculate  
Plume Centerline Temperature and  
Ceiling Jet Temperature with Experiments

---

---

William D. Davis



United States Department of Commerce  
Technology Administration  
National Institute of Standards and Technology

# NISTIR 6448

---

---

## Comparison of Algorithms to Calculate Plume Centerline Temperature and Ceiling Jet Temperature with Experiments

---

---

William D. Davis  
Fire Safety Engineering Division  
Building and Fire Research Laboratory  
National Institute of Standards and Technology

January 2000



**U.S. Department of Commerce**  
William M. Daley, Secretary  
**Technology Administration**  
Dr. Cheryl L. Shavers, Under Secretary for Technology  
**National Institute of Standards and Technology**  
Raymond G. Kammer, Director



## Contents

|   |    |
|---|----|
| Abstract .....  | 1  |
| 1. Introduction .....                                     | 1  |
| 2. Theory .....   | 2  |
| 2.1 Plume Centerline Temperature .....                    | 2  |
| 2.2 Ceiling Jet Algorithm .....                           | 3  |
| 3. Comparison of Model Predictions with Experiments ..... | 4  |
| 3.1 Ceiling height of 0.58 m .....                        | 5  |
| 3.2 Ceiling height of 1.0 m .....                         | 5  |
| 3.3 Ceiling Height of 2.7 m .....                         | 6  |
| 3.4 Ceiling Height of 10 m .....                          | 6  |
| 3.5 Ceiling Height of 15 m .....                          | 7  |
| 3.6 Ceiling Height of 22 m .....                          | 8  |
| 4. Summary .....  | 9  |
| 5. References .....                                       | 10 |



# Comparison of Algorithms to Calculate Plume Centerline Temperature and Ceiling Jet Temperature with Experiments

William D. Davis  
National Institute of Standards and Technology

## Abstract

The predictive capability of two algorithms designed to calculate plume centerline temperature (Evans) and maximum ceiling jet temperature (Davis et. al.) in the presence of a hot upper layer are compared with measurements from a series of experiments. In addition, comparisons are made using the ceiling jet algorithm in CFAST (version 3.1), the unconfined plume algorithm of Heskestad, and the unconfined ceiling jet algorithm of Alpert. The experiments included ceiling heights of 0.58 m to 22 m and heat release rates (HRR) of 0.62 kW to 33 MW. It was shown that the unconfined ceiling algorithms underpredicted the temperatures while the ceiling jet algorithm in CFAST overpredicted the temperature in the presence of a hot layer. With the combined uncertainty of the measurement and the calculation roughly equal to  $\pm 20\%$ , the algorithms of both Evans and Davis et. al. consistently provided predictions either close to or within this uncertainty interval for all fire sizes and ceiling heights.

## 1. Introduction

Recent experiments<sup>1</sup> have demonstrated the need for an improved predictive capability for both ceiling jet temperature and plume centerline temperature in draft curtained, high bay spaces when upper layers develop. Algorithms have been developed and tested using JET<sup>2</sup>, a modified version of the zone fire model LAVENT<sup>3</sup>, which are able to simulate plume centerline temperature and ceiling jet temperature for the experiments<sup>1</sup>. These algorithms have subsequently been included in CFAST (version 3.1)<sup>4</sup> in order to test their accuracy using this platform. This study compares the predictions of the algorithms for ceiling jet temperature (Davis et. al.<sup>2</sup>) and plume centerline temperature (Evans<sup>5</sup>) with the measurements from several experiments<sup>1,6,7,8,9</sup>. Also included in the comparisons are the ceiling jet predictions of CFAST (version 3.1), Alpert's unconfined ceiling jet algorithm<sup>10</sup> and the plume centerline temperature predictions of Heskestad's unconfined plume algorithm<sup>11</sup>.

The experiments selected for comparison with these models span a wide range of parameters including ceiling height and fire size. Since this work is done in the context of buildings, only experiments which formed a hot ceiling layer were used. In most instances, comparison between prediction and measurement is made after the growing fire has reached a steady-state heat release rate (HRR). Plume centerline temperature comparisons are made for ceiling heights ranging from 0.58 m to 22. m while ceiling jet temperature comparisons are made for ceiling heights ranging from 1.0 m to 22. m.

## 2. Theory

### 2.1 Plume Centerline Temperature

The analysis of fire plumes is based on the solution of the conservation laws for mass, momentum and energy. Early work centered on point sources and assumed that the air entrainment velocity at the edge of the plume was proportional to the local vertical plume velocity<sup>12</sup>. Measurements of plume centerline temperature in plumes with unconfined ceilings led to a correlation developed by Heskestad<sup>11</sup> which was consistent with theory. The correlation gives the excess temperature as a function of height above a virtual point source to be

$$\Delta T_p = 9.1 \left( \frac{T_\infty}{g c_p^2 \rho_\infty^2} \right)^{1/3} Q_c^{2/3} (z - z_0)^{-5/3} . \quad (1)$$

The virtual origin ( $z_0$ ) is given by

$$z_0 = -1.02D + 0.083Q^{2/5} \quad (2)$$

where  $Q$  and  $Q_c$  are the total and the convective heat release rates,  $D$  is the fire diameter,  $z$  is the height above the fire surface, and  $T_\infty$ ,  $c_p$ , and  $\rho_\infty$  are the temperature, heat capacity, and density of the ambient gas. When a hot upper layer forms, this correlation must be modified in order to predict plume centerline temperature since the plume now includes added enthalpy by entraining hot layer gas as it moves through the upper layer to the ceiling. Methods of defining a substitute virtual source and heat release rate in order to extend the plume into the upper layer have been developed by Cooper<sup>13</sup> and Evans<sup>5</sup>. Evans' method defines the strength  $Q_{i,2}$  and location  $Z_{i,2}$  of the substitute source with respect to the interface between the upper and lower layers by

$$Q_{i,2}^* = [(1 + C_T Q_{i,1}^{*2/3}) / \xi C_T - 1 / C_T]^{3/2} \quad (3)$$

$$Z_{i,2} = \left[ \frac{\xi Q_{i,1}^* C_T}{Q_{i,2}^{*1/3} [(\xi - 1)(\beta^2 + 1) + \xi C_T Q_{i,2}^{*2/3}]} \right]^{2/5} Z_{i,1} \quad (4)$$

$$Q_{l,1}^* = Q_c / (\rho_\infty C_\infty T_\infty g^{1/2} Z_{l,1}^{5/2}) \quad (5)$$

where  $Z_{l,1}$  is the distance from the fire to the interface between the upper and lower layer,  $Z_{l,2}$  is the distance from the virtual source to the layer interface,  $\xi$  is the ratio of upper to lower layer temperature,  $\beta$  is an experimentally determined constant<sup>14</sup> ( $\beta^2 = 0.913$ ),  $Z_{l,1}$  is the height from the fire to the layer interface, and  $C_T = 9.115$ . The distance between the virtual source and the ceiling,  $H_2$ , is then obtained from

$$H_2 = H_1 - Z_{l,1} + Z_{l,2} \quad (6)$$

where  $H_1$  is the location of the fire beneath the ceiling (see figure 1). The new values of the fire source and ceiling height are then used in a standard plume correlation<sup>15</sup> where the ambient temperature is now the temperature of the upper layer. The plume excess temperature is given by

$$\Delta T_p = 9.28 T_u (Q_{l,2}^*)^{2/3} \left( \frac{Z_{l,2}}{H_2} \right)^{5/3} \quad (7)$$

where  $T_u$  is the temperature of the upper layer.

## 2.2 Ceiling Jet Algorithm

The ceiling jet temperature algorithm (Davis et. al.<sup>2</sup>) predicts the maximum temperature excess of the ceiling jet in the presence of a growing upper layer. The ceiling jet temperature excess as a function of radius for  $r/H > 0.18$  is given by

$$\Delta T = k \Delta T_p \left( \frac{r_o}{r} \right)^\gamma, \quad (8)$$

where

$$k = (0.68 + 0.16(1 - e^{-y_l/y_j})) \quad (9)$$



$$r_o = 0.18H, \quad (10)$$

$$\gamma = 2/3 - \alpha(1 - e^{-y_L/y_j}), \quad (11)$$

and  $\alpha = 0.44$ ,  $y_j = 1.0$  m,  $y_L$  is the layer thickness, and  $\Delta T_p$  is the plume centerline temperature excess as calculated using Evans' method (equations 3 - 8). When a hot layer is not present, the model reduces to the correlation of Alpert<sup>5</sup> for  $r/H > 0.18$  with the exception that the convective heat release rate rather than the total heat release is used in the correlation.

$$\Delta T = 5.4 \frac{\left(\frac{Q_c}{r}\right)^{2/3}}{H} \quad (12)$$

A modification was made to this algorithm in order to accommodate the low ceiling heights modeled in this paper. The parameter  $y_j$ , which was given a constant value of 1.0 m in reference 2, was changed to  $0.1 * H$  such that the algorithm could handle ceiling heights from 0.58 m to 22 m.

### 3. Comparison of Model Predictions with Experiments

Data from a series of experiments was obtained for the purpose of comparison with the predictions of the algorithms described in section 2. A brief description of each experiment will be included in the sections below. The experiments will be organized according to the distance between the fire source and the ceiling with the range being 0.58 m to 22 m. The new algorithms for ceiling jet temperature and plume centerline temperature using CFAST as the computational base will be designated as DNT in the comparisons, while the present ceiling jet algorithm in CFAST, version 3.1 will be designated as v3.1.

Uncertainty intervals are provided for both experimental measurements and model predictions. For each experiment, the experimental uncertainties are either those given in the report or are estimated based on the experimental data and fire type.

Computer fire models require a number of experimentally determined input values and the uncertainty in each input value generates an uncertainty in the calculated result. Uncertainty intervals for the models in this paper are based on the estimated uncertainty in the convective heat release rate. Uncertainties in the measurement of the distance between the fire and the ceiling, and the material properties of the walls and ceiling are neglected. The uncertainty in convective heat release rate is equal to the combined uncertainty for the HRR and the radiative fraction. The uncertainty intervals for the calculations were obtained by using a high, middle and low estimate of the convective heat release rate. These estimates were done either by varying the radiative fraction

or by varying the total heat release rate. Since the convective heat release rate,  $HRR_c$ , is given by

$$HRR_c = (1 - \chi_r) * HRR , \quad (13)$$

varying either the radiative fraction,  $\chi_r$ , or the HRR will have the same effect on  $HRR_c$ . Predictions and measurements are judged to be in agreement when the uncertainty intervals overlap. While it is tempting to compare the measured and predicted values and ignore the uncertainty intervals, the uncertainty intervals are a guide to the accuracy of a measurement or model prediction. There are six experiments against which the new algorithms, as well as previous algorithms, are compared.

### 3.1 Ceiling height of 0.58 m

A cylindrical enclosure of 1.22 m diameter formed by a 0.29 m deep PMMA curtain around a 13 mm thick ceramic fiber board ceiling was used to study the temperature produced by an axisymmetric plume. The fire source was a methane gas burner of diameter 0.0365 m located at the center of the cylinder. The top of the burner was located 0.58 m beneath the ceiling. The heat release rate was 0.62 kW. Details of this experiment are available in reference 6.

This experiment measured plume centerline temperature as a function of height but not ceiling jet temperature. Figure 2 compares the predicted plume centerline temperature using DNT and Heskestad's correlation with the measured value. Uncertainty intervals for the measurements were given in the reference while the uncertainty in the calculations represent an estimation of the uncertainty in the HRR of the experiment of  $\pm 5\%$ . The plume centerline temperature predicted using DNT lies within the combined uncertainty interval of the measurement and the calculation. Heskestad's correlation substantially underpredicts the plume centerline temperature which is expected in situations where hot layers form.

### 3.2 Ceiling height of 1.0 m

A cylindrical enclosure of diameter 2.13 m formed by a 0.5 m deep corrugated cardboard curtain around a 1.27 cm thick fiberboard ceiling was used to study the development of a ceiling jet at distances of  $r/H = 0.26$  and  $r/H = 0.75$  where  $r$  is the radial distance from the fire center and  $H$  is the distance between the burner outlet and the ceiling. The fire consisted of a methane flame produced using a 2.7 cm diameter burner. The burner outlet was located at the center of the cylindrical enclosure and was 1.0 m below the ceiling. The fire sizes used in this study were 0.75 kW and 2.0 kW. Additional details concerning this experiment can be found in reference 7.

Figures 3 and 4 gives the predictions of the new algorithms (DNT) and version 3.1 of CFAST (v3.1) compared with the ceiling jet temperature maximums. There was no guidance given by the authors concerning the uncertainties of their measurements. It was assumed that an uncertainty interval of

$\pm 10\%$  would be a reasonable approximation of the measurement accuracy which would include systematic errors and data scatter in the temperature measurements, the burner flow rates, combustion efficiency, and radiative fraction of the fuel source. The DNT ceiling jet algorithm predicted the ceiling jet temperature within the combined uncertainties of the calculations and the measurements although the trend for both fire sizes was to underpredict the temperature. The algorithm in version 3.1 of CFAST predicted the ceiling jet temperature at  $r/H = 0.26$  within the combined uncertainties but overpredicted the temperature at  $r/H = 0.75$ . Albert's ceiling jet correlation substantially underpredicted the temperature at both radial positions.

### **3.3 Ceiling Height of 2.7 m**

A series of experiments were conducted using a ceiling measuring 9.75 m x 14.6 m. Simulated beams, 0.305 m deep and separated by 1.22 m, were installed on the ceiling with the beams parallel to the long dimension of the ceiling. A pair of experiments (tests 7 & 4), one with a 1.22 m deep draft curtain and one without a draft curtain, were chosen for the analysis. Wood cribs were used as the fire source with the bottom of the beams located 2.43 m above the top of the wood cribs. Since the growth rate of the fire as a function of time was provided, comparisons were made at several different fire sizes. The fire sizes for these comparisons ranged from 30 kW to 830 kW. Additional information concerning the experiments can be found in reference 8.

Figure 5 and 6 display the comparison between the computer predictions, Heskestad's plume correlation, and the measurements for the plume centerline temperature for test 4 which contained 0.305 m deep beams and test 7 which included the ceiling beams plus a 1.22 m deep draft curtain. The uncertainty intervals used for the data are estimated to be  $\pm 5\%$  while the calculations were done by taking the reported time dependent heat release rate and varying the radiative fraction between 0.20 and 0.45. The temperatures are calculated using a radiative fraction of 0.35. As the fire size increases and the layer develops, the predictions of DNT provide better agreement than the correlation of Heskestad. At the largest fire size, both models significantly underpredict the plume centerline temperatures.

Several reasons may combine to produce the significant underprediction at the largest fire sizes for these experiments. First, the combustion region of the flame is approaching the ceiling for the larger fires. The plume algorithms used in these comparisons are valid only out of the combustion region and hence when the flames get close to the ceiling, the accuracy of the plume algorithm comes into question. Second, since the combustion region is close to the ceiling, the radiation to the ceiling and hence to the thermocouple becomes significant. The thermocouple reading would require correction for radiation effects which would effectively lower the measured temperature. This was not done in the experiments. Third, as the fire size increases, the radiative fraction may decrease with fire size as the fire volume becomes optically thick. This effect was not included in the calculations.

### **3.4 Ceiling Height of 10 m**

A series of experiments were conducted in a building with a space of 53 m x 22 m x 11.3 m high. A 2 m square hexane fire produced a heat release rate of 4.6 MW. The convective heat release rate was estimated to be 3.05 MW. The roof was carried on 1 m deep timber beams and a draft curtain 3.2 m deep as measured from the bottom of the beams divided the building into two spaces. A false level ceiling 10 m above the floor was attached to the bottom of the beams in the space where the experiments were conducted. Additional information concerning the experiments can be found in reference 9.

Shown in figure 7 are comparisons of the estimated plume centerline temperature to the predictions of DNT and Heskestad's plume algorithm. The uncertainties for the radial temperature measurements, as provided by the authors, was  $\pm 4$  °C. The uncertainties for the calculations are based on the assumption that the radiative fraction of the fuel varied from 0.25 to 0.40. The calculated values are based on a radiative fraction of 0.34 which was given by the authors. The uncertainty used for the radiative fraction is designed to include the uncertainty in the heat release rates, radiative fraction and thermal losses to the ceiling. From the figure, DNT overpredicts the plume centerline temperature while Heskestad's plume algorithm predicts the centerline temperature within the uncertainty intervals. Since this experiment formed a deep hot layer, the agreement of the plume centerline temperature with Heskestad's algorithm is surprising. One explanation for this result is that the experiment may not have had enough thermocouples in the plume region to resolve the plume centerline temperature. It was noted that the plume centerline wandered in location and typically was located some distance away from the fire centerline. The plume centerline temperature used in this comparison was extrapolated from a radial temperature dependence plot which did not include a temperature at the plume centerline. Hence, the plume centerline temperature may have been higher than was actually reported in the experiment.

Figure 8 gives the comparison between the ceiling jet temperature predictions of the DNT, CFAST V3.1, Alpert's ceiling jet algorithm and the measured values. The values predicted by DNT lie within the combined uncertainty interval. Since the results of this model depends on predicting the plume centerline temperature accurately, this comparison lends support to the supposition that the measured plume centerline temperature for this experiment is low. The ceiling jet temperature predictions of V3.1 are substantially higher than the measured values. The ceiling jet temperatures predicted by Alpert's model are substantially lower than measured which is expected when a deep hot layer develops.

### **3.5 Ceiling Height of 15 m**

A series of JP-5 pool fires were conducted in a hangar of size 97.8 m x 73.8 m x 15.1 m. The fires were centered under a draft curtained area 18.3 m x 24.4 m with a ceiling height of 14.9 m. The draft curtain was 3.7 m deep. Three JP-5 pool fire experiments, a 0.61 m square 0.48 MW fire, a 1.5 m diameter 2.8 MW fire and a 2.5 m diameter 7.7 MW fire, were modeled. Additional information concerning these experiments can be found in reference 1.

Figure 9 gives the comparisons of the plume centerline temperature predictions of DNT and Heskestad's plume algorithm with the measured values. DNT predicts the temperature within the uncertainty intervals for the two smaller fires while Heskestad's algorithm provides predictions within the uncertainty interval for all three fires. The heat release rate for the 7.7 MW fire was determined by a fuel mass loss method rather than direct load cell measurements which, due to fuel evaporation at the end of the experiment, may lead to an overestimation of HRR but there was no way to determine how much of an overestimate is involved in the measurement.

The uncertainty interval for the measurements were based on the measured RMS temperature fluctuations and are equal to  $\pm\sigma$ . The uncertainty interval for the calculations was determined by varying the HRR  $\pm 15\%$ . This uncertainty should include the uncertainty in the radiative fraction as well as the uncertainty in the HRR. The uncertainty in the HRR was not increased for the 7.7 MW fire.

Figures 10 and 11 give the comparisons of the ceiling jet temperature predictions of DNT and version 3.1 with the measured values. Only the 2.7 MW fire and the 7.7 MW were used in the comparison owing to the small temperature excess in the ceiling jet for the 0.48 MW experiment. The temperature predictions of DNT were within the combined uncertainty interval for the 2.7 MW experiment and for the 3.1 m position in the 7.7 MW experiment. The temperatures at the 6.1 m and 9.1 m positions for the 7.7 MW fire were under predicted by DNT. Version 3.1 of CFAST overpredicted all locations for both experiments except for the 3.1 m position of the 2.7 MW fire. The uncertainty intervals for the ceiling jet temperatures were treated in the same manner as for the plume centerline temperatures.

### **3.6 Ceiling Height of 22 m**

A series of JP-5 and JP-8 pool fires were conducted in a hangar of size 73.8 m x 45.7 m and had a barrel roof which was 22.3 m high at the center and 12.2 m high at the walls. Corrugated steel draft curtains were used to divide the ceiling into five equal bays approximately 14.8 m x 45.7 m with the fire experiments conducted in the middle bay and centered under the 22.3 m high ceiling. Nine experiments with fire sizes ranging from 1.4 MW to 33 MW were modeled. Additional information concerning these experiments can be found in reference 1.

Figure 12 gives the comparison of the plume centerline temperature predictions of DNT and Heskestad's correlation with the measured values. These experiments produced the deepest hot layers and the presence of these hot layers can be seen in the general underprediction of Heskestad's correlation when compared with the measurements. The predictions of DNT were within the uncertainty intervals for all the experiments. The uncertainty intervals for the measurements were based on the measured RMS temperature fluctuations and are equal to  $\pm\sigma$ . The uncertainty interval for the calculations was determined by varying the HRR  $\pm 15\%$ . This uncertainty should include the uncertainty in the radiative fraction as well as the uncertainty in the HRR.

Figures 13 - 19 give the comparison of the ceiling jet temperature predictions of DNT and version

3.1 with the measured values at distances of 6.1 m, 9.1 m, and 12.2 m from plume center. These measurements were along the curved part of a barrel roof. The predictions of DNT were within or slightly above the uncertainty interval for the measured values while the predictions of version 3.1 were substantially above the measured values. The uncertainty intervals for the ceiling jet temperatures were treated in the same manner as for the plume centerline temperatures.

#### **4. Summary**

New algorithms for the calculation of plume centerline temperature and ceiling jet temperature have been tested in CFAST for a number of experiments with different ceiling heights, draft curtain depths and fuel types. Evans' plume centerline temperature algorithm, implemented in DNT, predicted temperatures which were within the combined uncertainty interval for the measurement and calculation for eleven of the sixteen experiments in which centerline temperatures were measured as shown in figure 20. In general, the combined uncertainty interval can be taken as equal to  $\pm 20\%$ . The maximum error was roughly 25% for all sixteen comparisons. Heskestad's correlation underpredicted the plume centerline temperature by more than 20% in ten of the sixteen experiments with six experiments being underpredicted by more than 30%. Heskestad's plume algorithm is designed for unconfined ceilings where a hot layer is not expected to form and hence the underpredictions are expected. Evans' algorithm systematically overpredicted most of the temperatures. The tendency for this algorithm to overpredict the temperature may be the result of a choice of constants in the plume algorithm or it may result from the layer temperature calculation in CFAST.

The ceiling jet algorithm, DNT, performed extremely well, predicting ceiling jet temperatures within the combined uncertainty interval for eleven of twelve experimental comparisons as shown in figure 21. The algorithm gave substantially better predictions than the present algorithm used in version 3.1 of CFAST which overpredicted the ceiling jet temperature by 20% or more in all twelve experiments or Alpert's correlation which underpredicted the ceiling jet temperature in all twelve experiments by 20% or more. Since the ceiling jet temperature was compared in a number of locations for every experiment, the percent difference given in figure 20 is based on an average error over the positions of comparison for each experiment.

## 5. References

1. Gott, J. E., Lowe, D. L., Notarianni, K. A., and Davis, W. D., "Analysis of High Bay Hangar Facilities for Detector Sensitivity and Placement," National Institute of Standards and Technology, *NIST Technical Note 1423*, Gaithersburg, MD (1997) pp. 1 -315.
2. Davis, W. D., "The Zone Fire Model JET: A Model for the Prediction of Detector Activation and Gas Temperature in the Presence of a Smoke Layer", NISTIR 6324, 1999, pp. 1 - 51.
3. Davis, W. D., and Cooper, L. Y., "Estimating the Environment and the Response of Sprinkler Links in Compartment Fires with Draft Curtains and Fusible Link-Actuated Vents - Part II: User Guide for the Computer Code LAVENT," *National Institute of Standards and Technology*, NISTIR 89-4122, 1989, pp.1 - 36.
4. Peacock, R. D., Reneke, P. A., Jones, W. W., Bukowski, R. W. and Forney, G. P., "A User's Guide for FAST: Engineering Tools for Estimating Fire Growth and Smoke Transport", *National Institute of Standards and Technology*, Special Publication 921, 1997, pp. 1 - 180.
5. Evans, D. D., "Calculating Sprinkler Actuation Time in Compartments," *F. Safety J.*, 9, 1985, pp. 147 - 155.
6. Evans, D. D., "Calculating Fire Plume Characteristics in a Two Layer Environment", *Fire Technology*, 20, No. 3, 1984, pp. 39 - 63.
7. Montevalli, V. and Ricciuti, C., "Characterization of the Confined Ceiling Jet in the Presence of an Upper Layer in Transient and steady-State Conditions", *National Institute of Standards and Technology*, NIST-GCR-92-613, 1992, pp. 1 - 134.
8. Heskestad, G., and Delichatsios, M. A., "Environments of fire Detectors - Phase II: Effect of Ceiling Configuration. Volume II. Analysis", *National Institute of Standards and Technology*", NBS-GCR-78-129, 1978, pp. 1 - 100.
9. Hinkley, P. L., Hansell, G. O., Marshall, N. R., and Harrison, R., "Large-Scale Experiments with Roof Vents and Sprinklers Part 1: Temperature and Velocity Measurements in Immersed Ceiling Jets Compared with a Simple Model", *Fire Science & Technology*, Vol. 13, No. 1 & No. 2., 1993, pp. 19 - 41.
10. Alpert, R. L., "Calculation of Response Time of Ceiling-Mounted Fire Detectors," *Fire Technology*, 8, 1972, pp. 181 - 195.
11. Heskestad, G., "Engineering Relations for Fire Plumes", *Fire Safety J.*, 7, 1984, pp.25 -32.
12. Morton, B. R. , Taylor, B. I., and Turner, J. D., "Turbulent Gravitational Convection from

- Maintained and Instantaneous Sources," *Proc. Roy. Soc.* A234, 1956, pp. 1 - 23.
13. Cooper, L. Y., "Fire-Plume-Generated Ceiling Jet Characteristics and Convective Heat Transfer to Ceiling and Wall Surfaces in a Two-Layer Zone-Type Fire Environment," *National Institute of Standards and Technology*, NISTIR 4705, 1991, pp. 1 - 32.
  14. Zukoski, E. E., Kubota, T., and Cetegen, B., "Entrainment in fire plumes," *Fire Safety J.*, 3, 1980, pp. 107-121.
  15. Heskestad, G., and Delichatsios, M. A., "The initial Convective Flow in Fire," *17 th International Symposium on Combustion*, Combustion Institute, Pittsburgh, 1978, pp. 1113 - 1123.



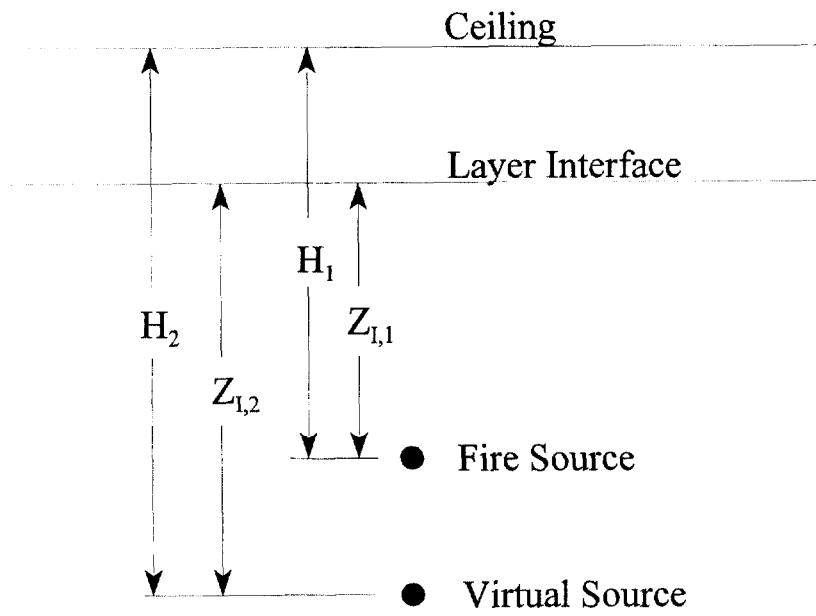


**Figure 1** Graphical representation of the relationship between the Fire Source ( $Q_{1,1}$ ) and the Virtual Source ( $Q_{1,2}$ ).

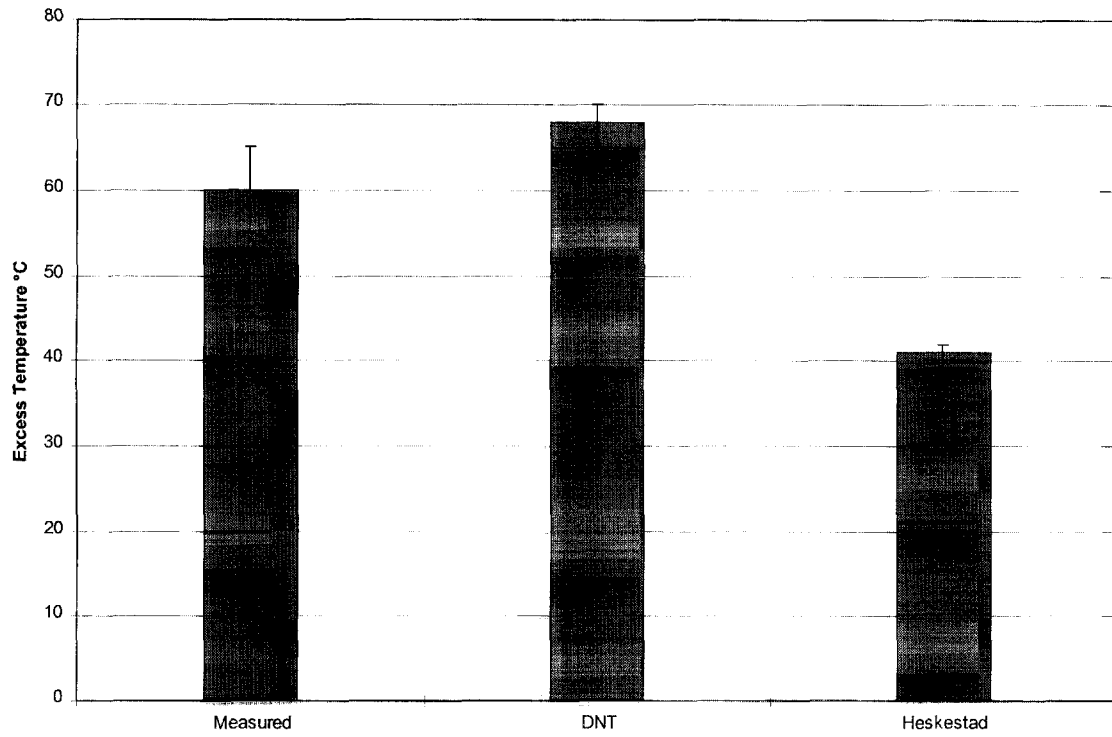


**Figure 2** Measured and predicted plume centerline temperature excess for the 0.58 m experiment.

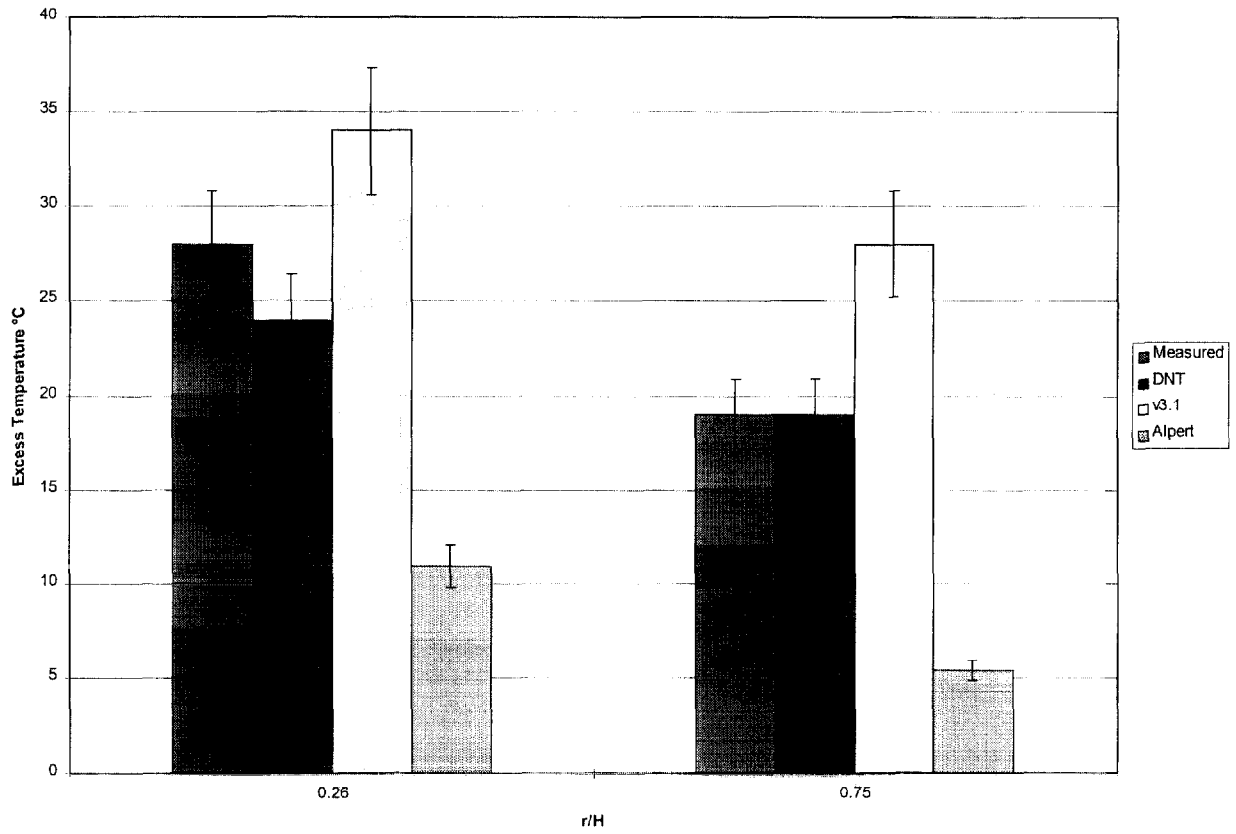


**Figure 3** Measured and predicted ceiling jet temperature excess at  $r/H = 0.26$  and  $0.75$  for the  $0.75$  kW,  $1.0$  m experiment.

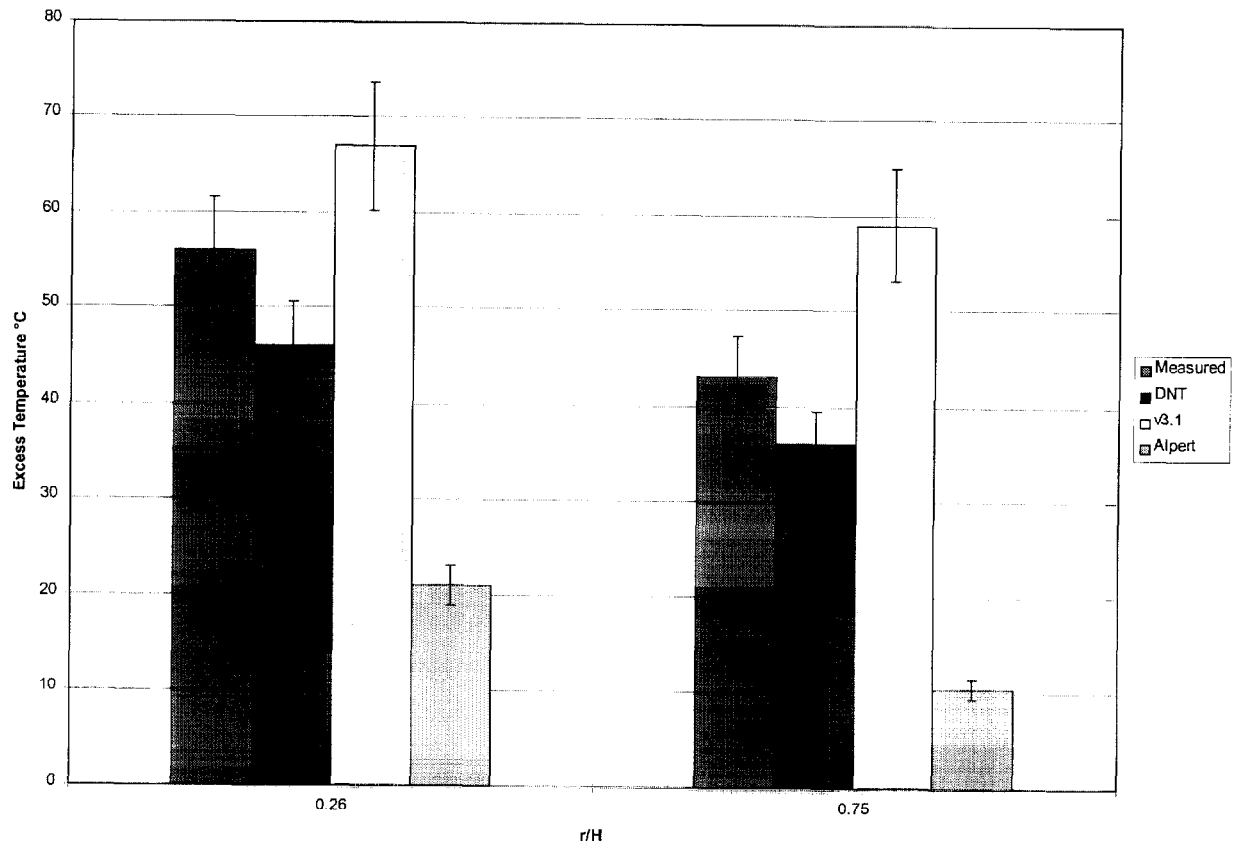


**Figure 4** Measured and predicted ceiling jet temperature excess at  $r/H = 0.26$  and  $r/H = 0.75$  for the 2.0 kW, 1.0 m experiment.

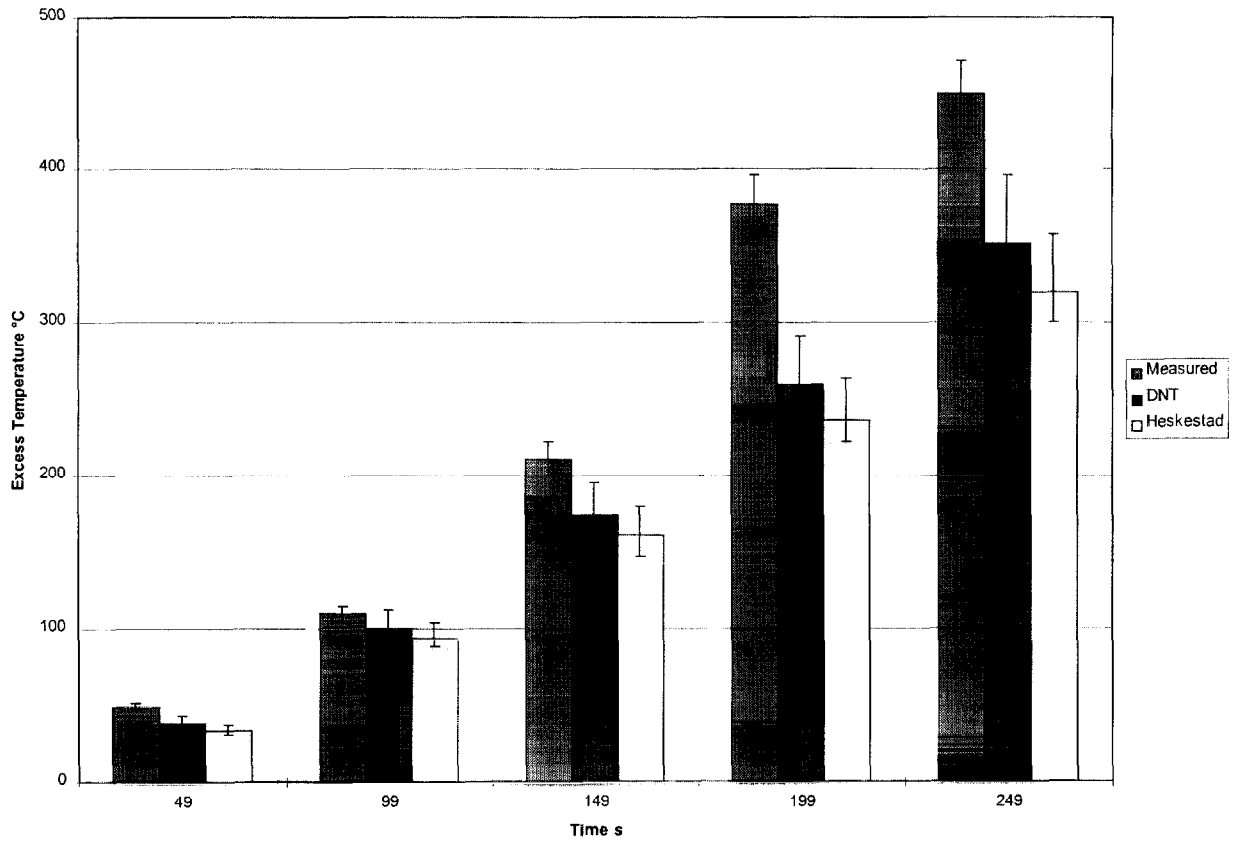


**Figure 5** Measured and predicted plume centerline temperature excess during the growing phase of the fire for the 2.7 m experiment without draft curtains.

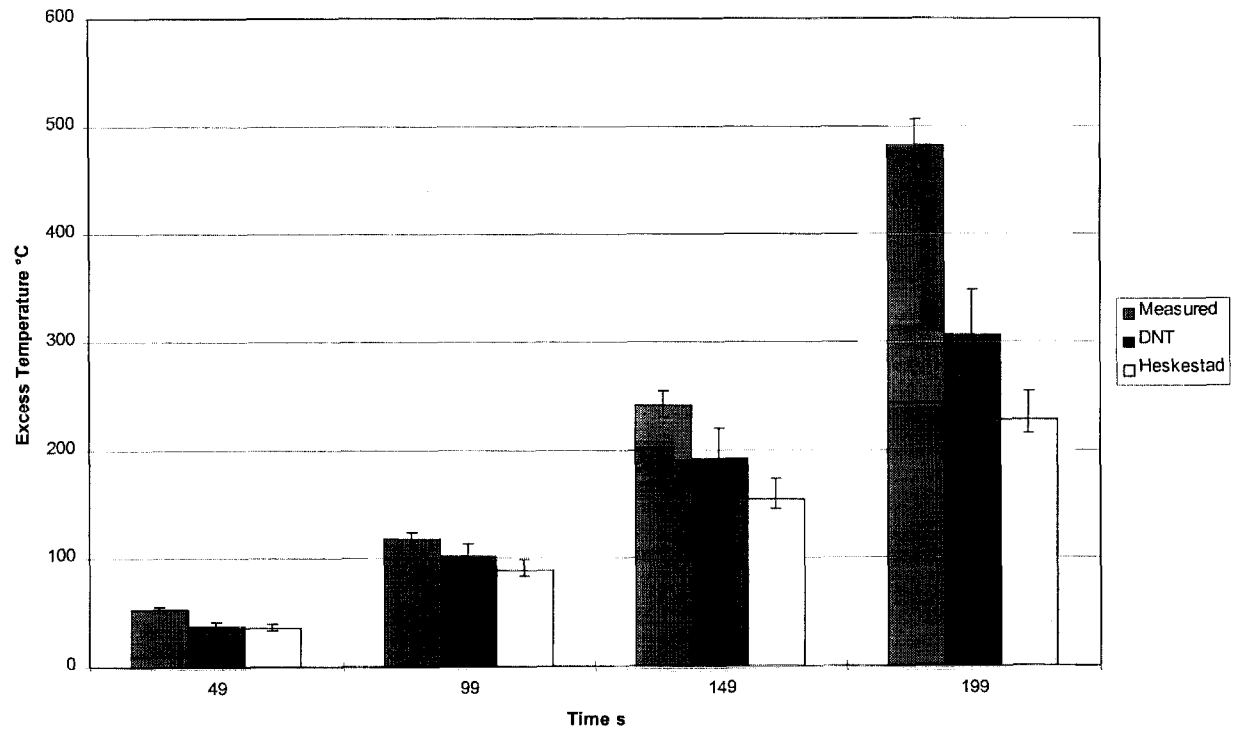


**Figure 6** Measured and predicted plume centerline temperature excess during the growing phase of the fire for the 2.7 m experiment with draft curtain.

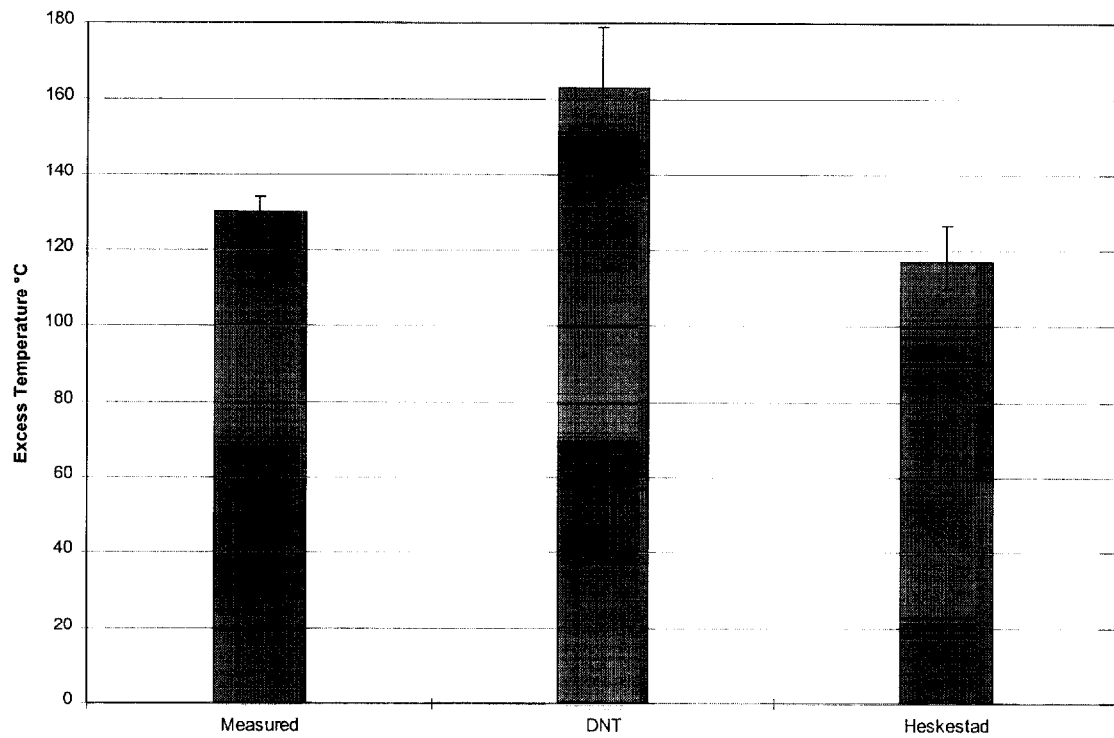


**Figure 7** Measured and predicted plume centerline temperature excess for the 10 m experiment

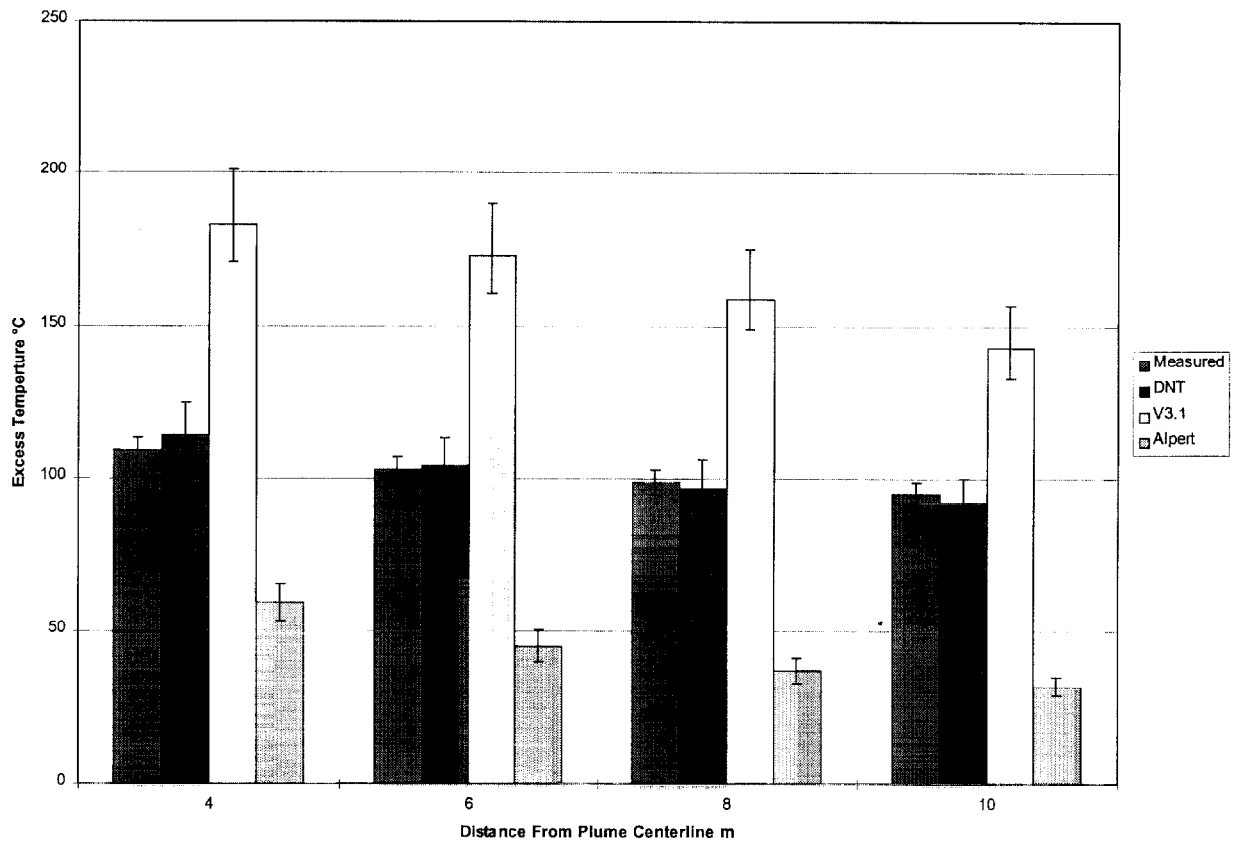


**Figure 8** Measured and predicted ceiling jet temperature excess for the 10 m experiment.



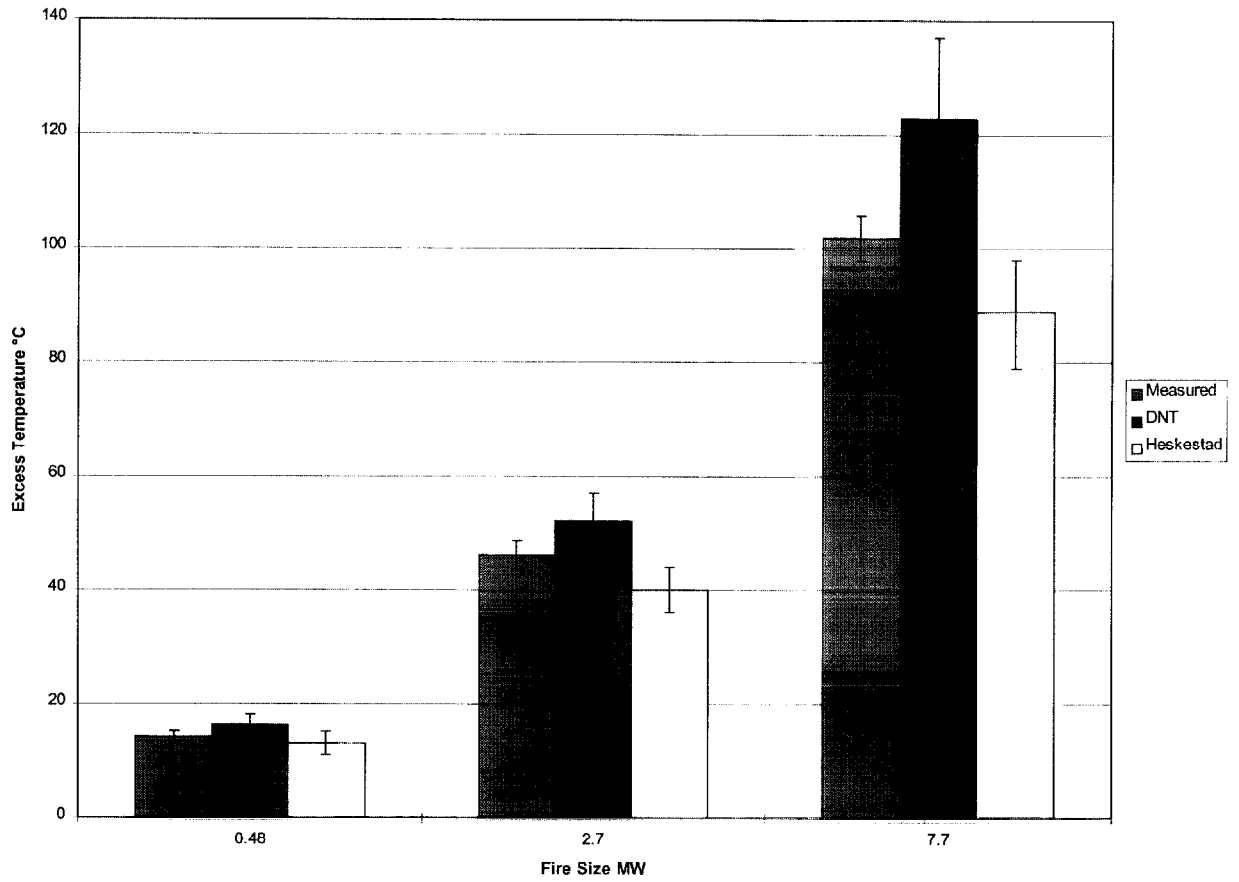


**Figure 9** Measured and predicted plume centerline temperature excess for the 15 m experiment.

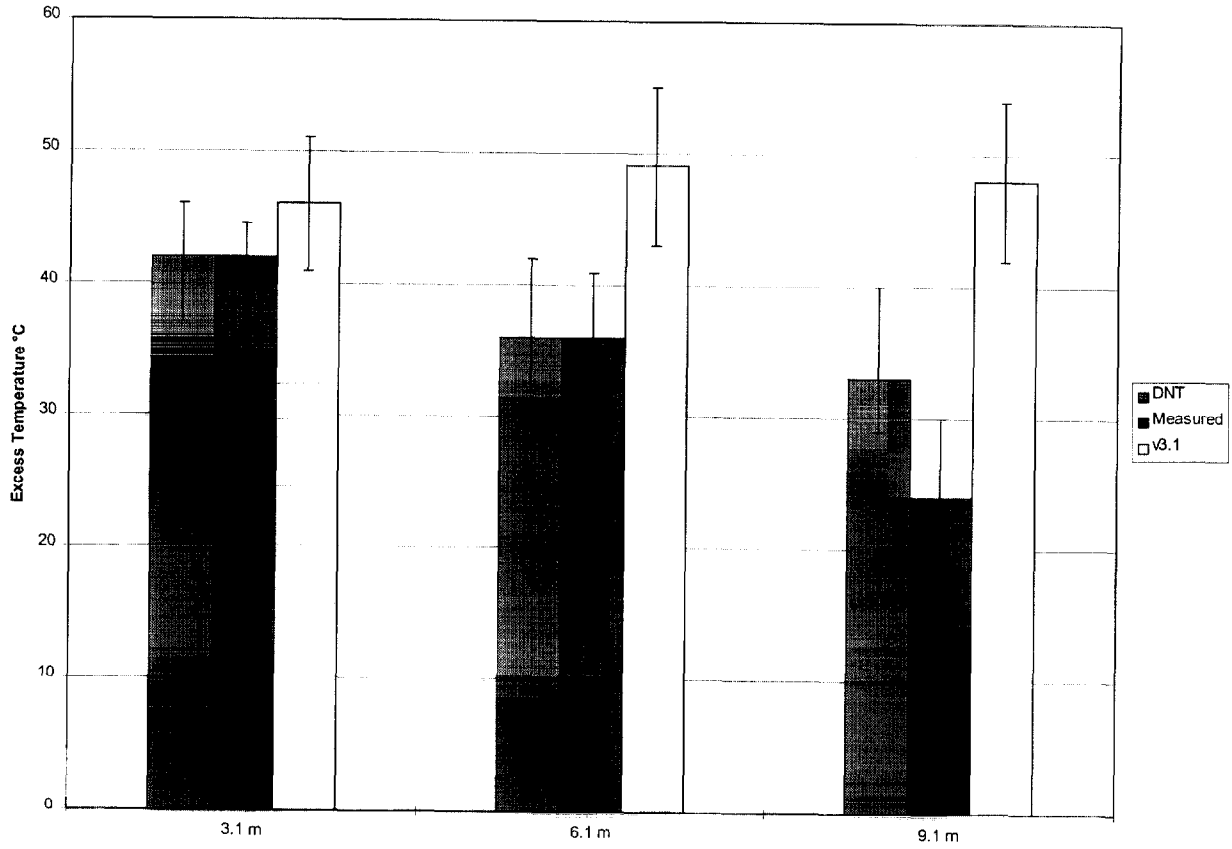


**Figure 10** Measured and predicted ceiling jet temperature excess for the 2.7 MW, 15 m experiment. Distances are measured radially from plume centerline.

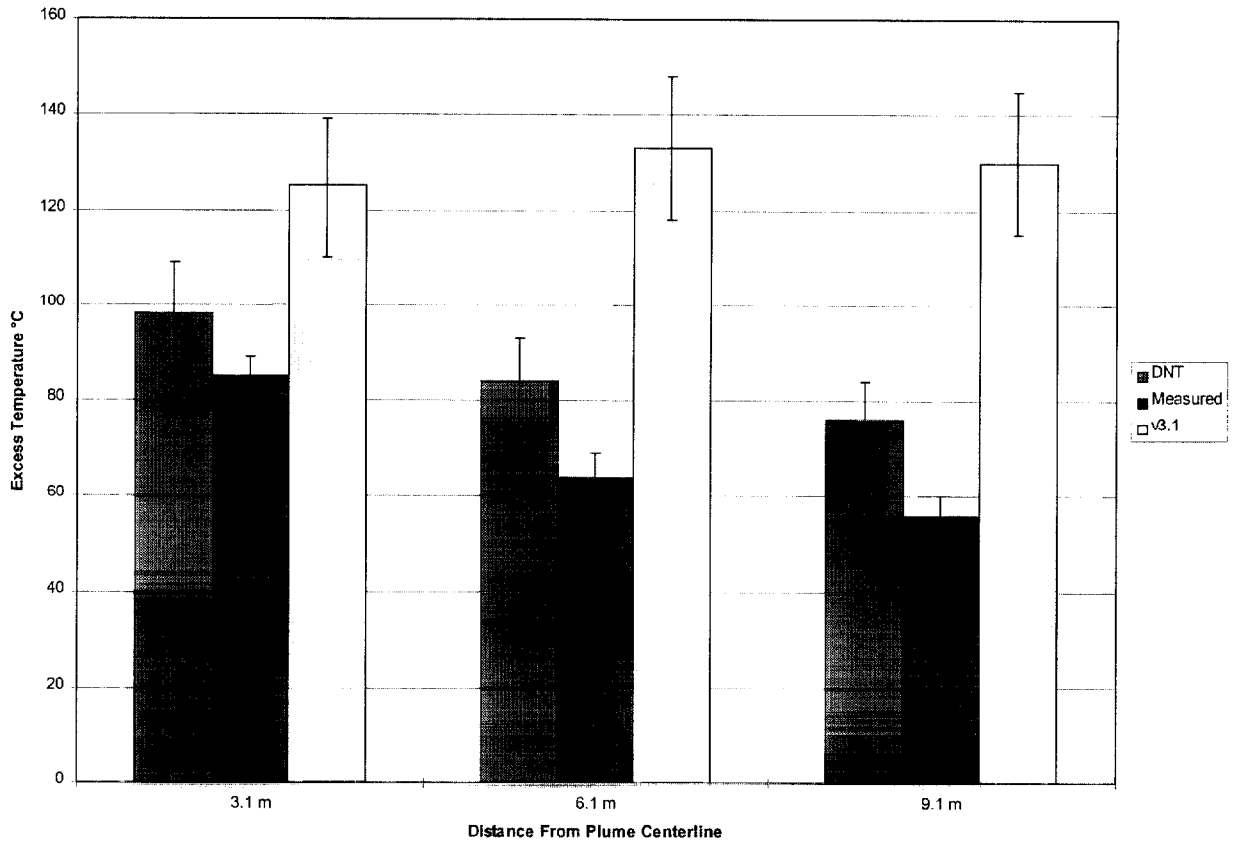


**Figure 11** Measured and predicted ceiling jet temperature excess for the 7.7 MW, 15 m experiment.

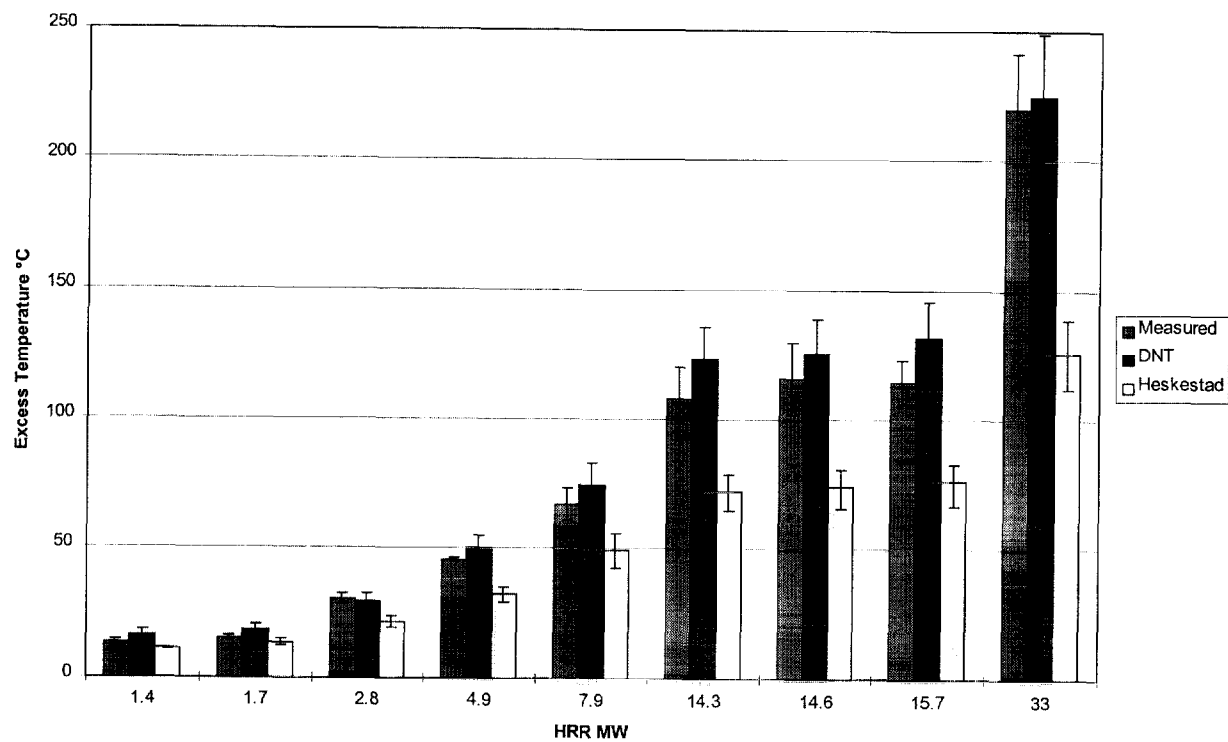
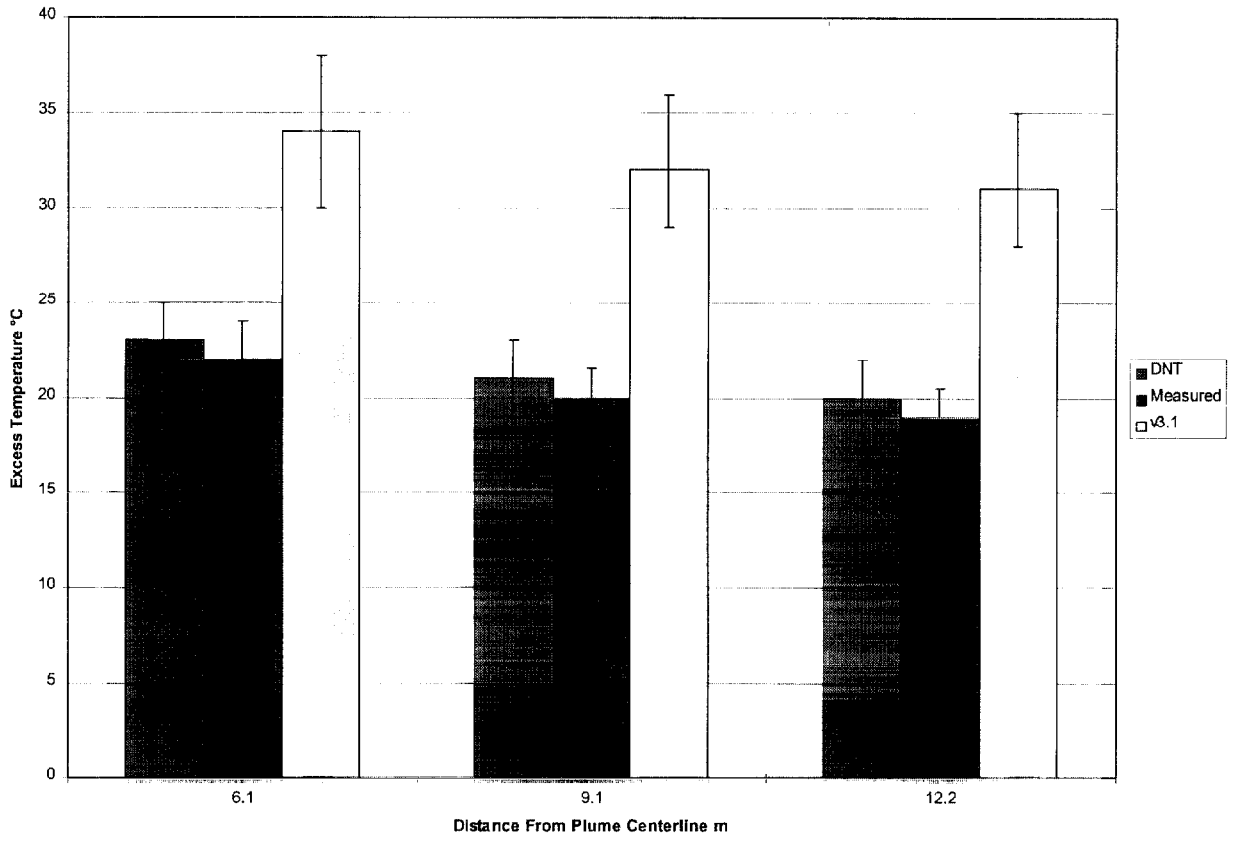
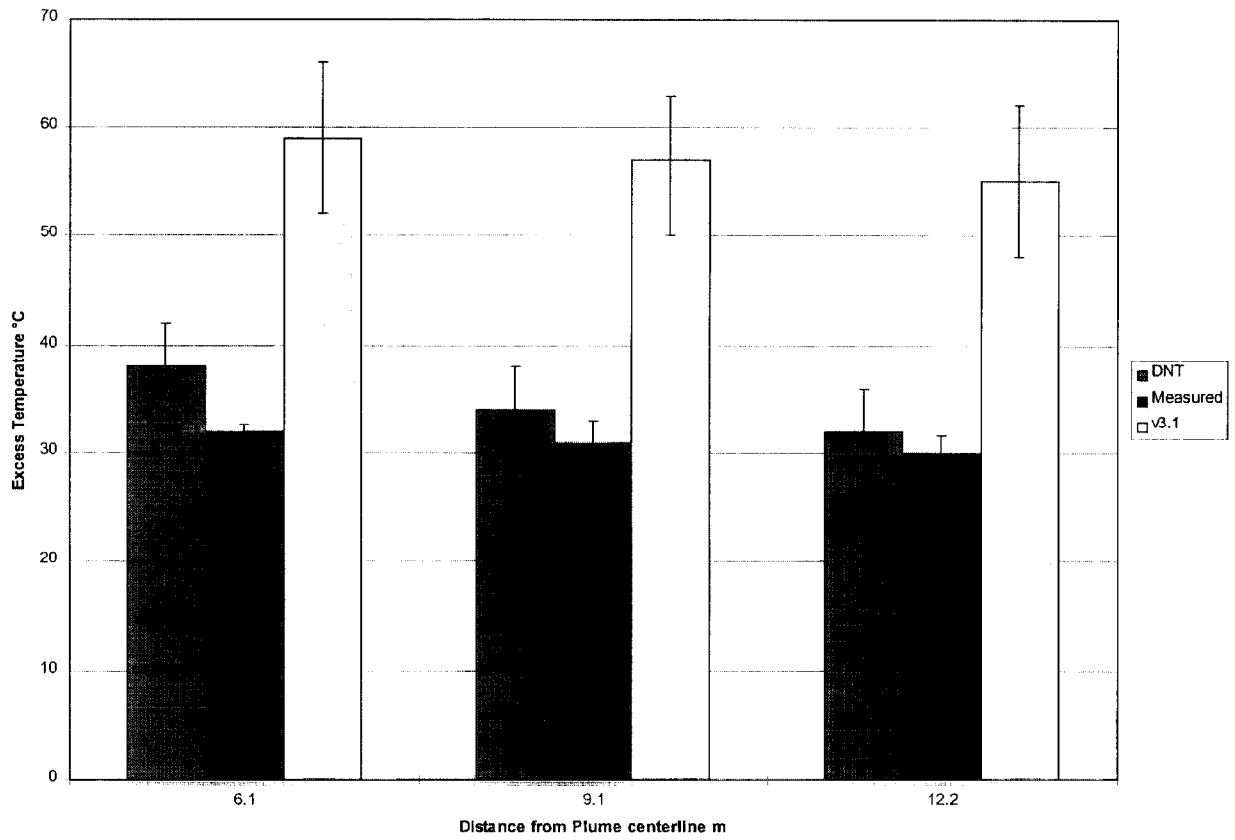


Figure 12 Measured and predicted plume centerline temperature excess for the 22 m experiment.



**Figure 13** Measured and predicted ceiling jet temperature excess for the 2.8 MW, 22 m experiment.



**Figure 14** Measured and predicted ceiling jet temperature excess for the 4.9 MW, 22 m experiment

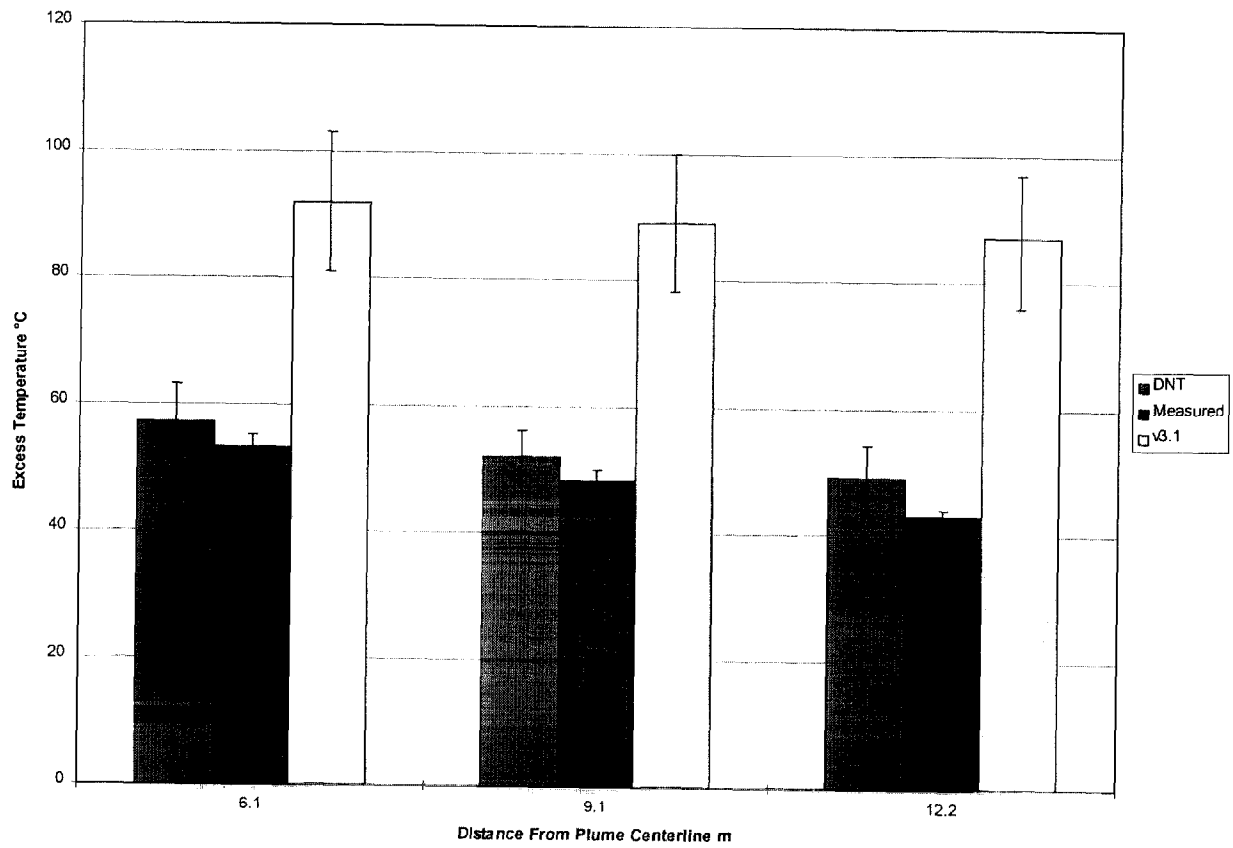


**Figure 15** Measured and predicted ceiling jet temperature excess for the 7.9 MW, 22 m experiment.

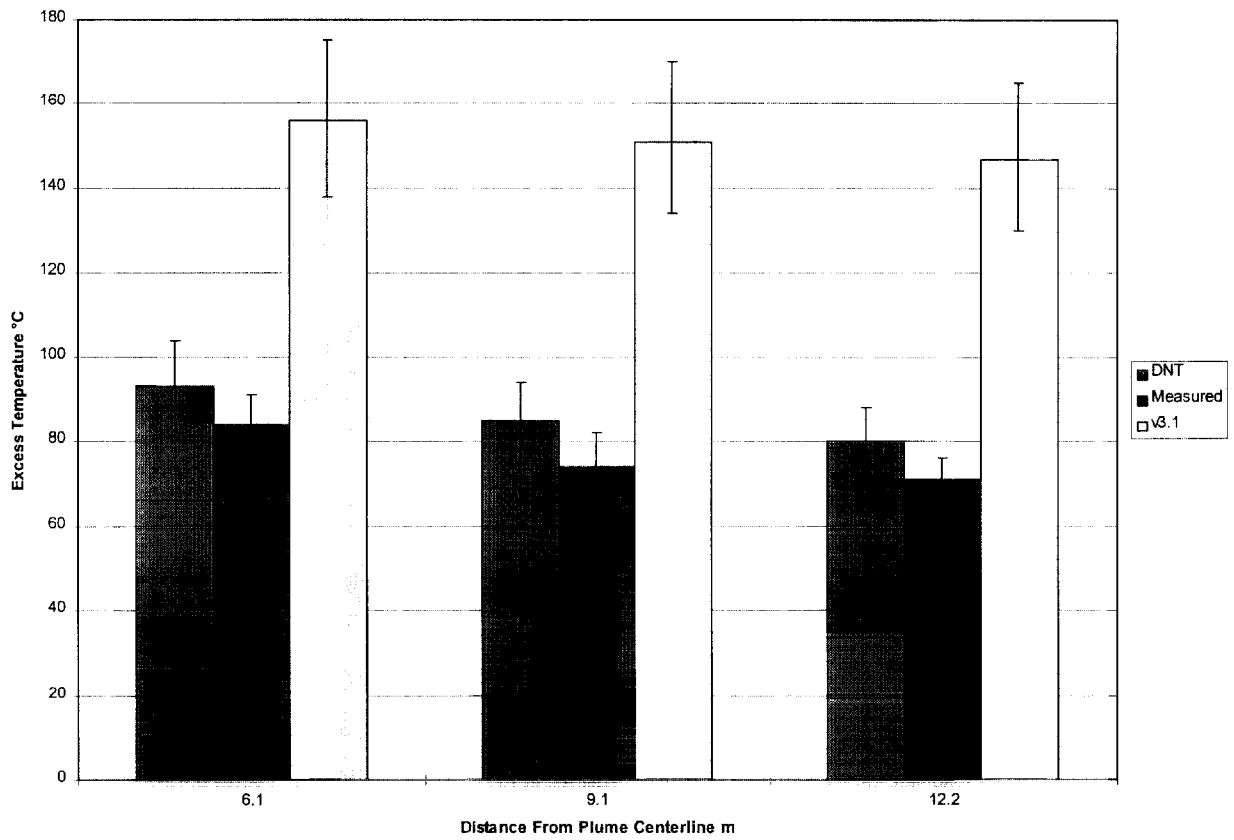


**Figure 16** Measured and predicted ceiling jet temperature excess for the 14.3 MW, 22 m experiment.



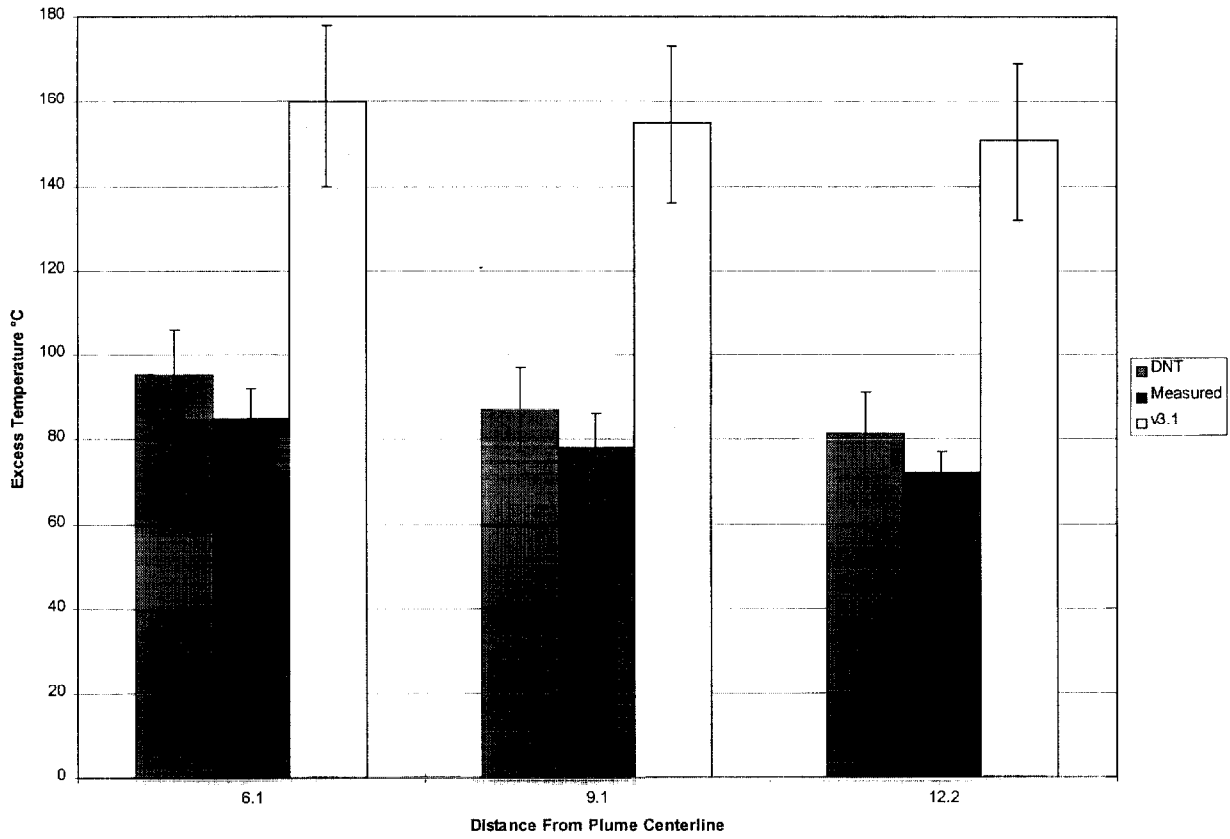


**Figure 17** Measured and predicted ceiling jet temperature excess for the 14.6 MW, 22 m experiment.

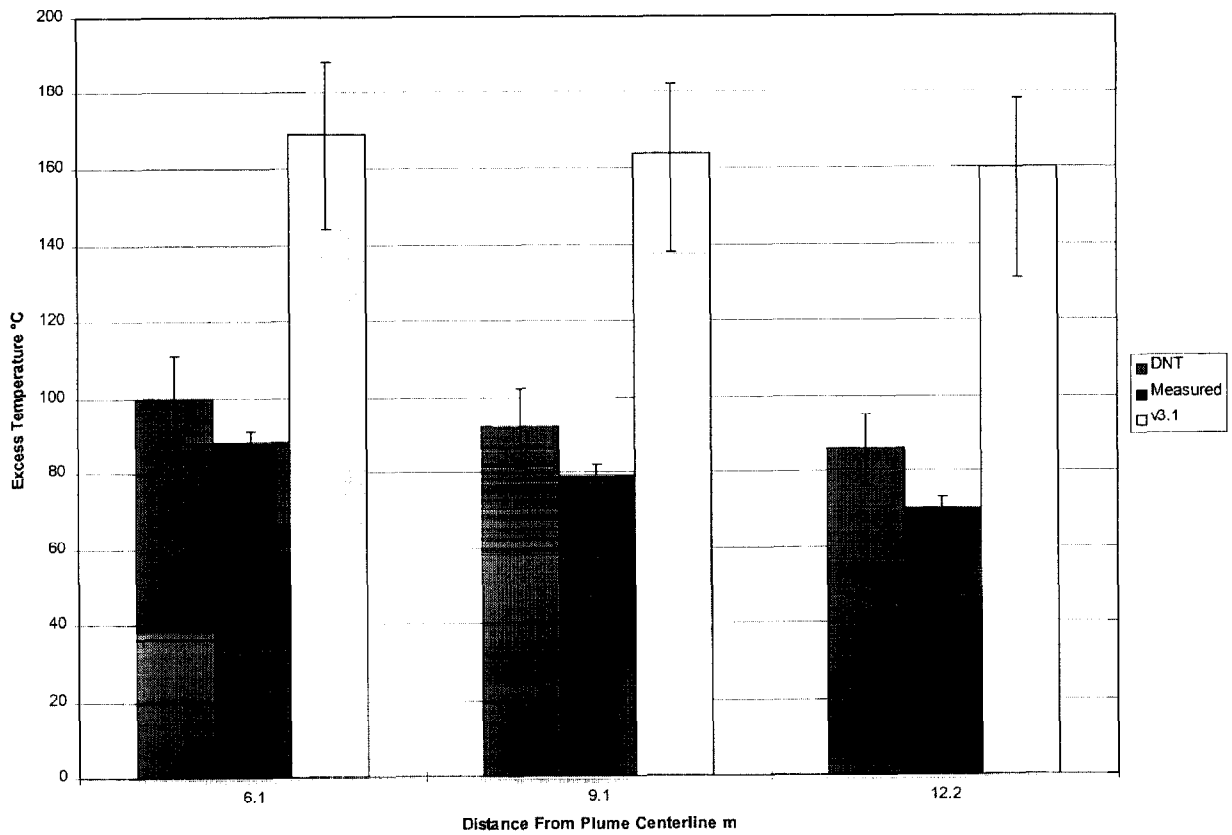


**Figure 18** Measured and predicted ceiling jet temperature excess for the 15.7 MW, 22 m experiment.

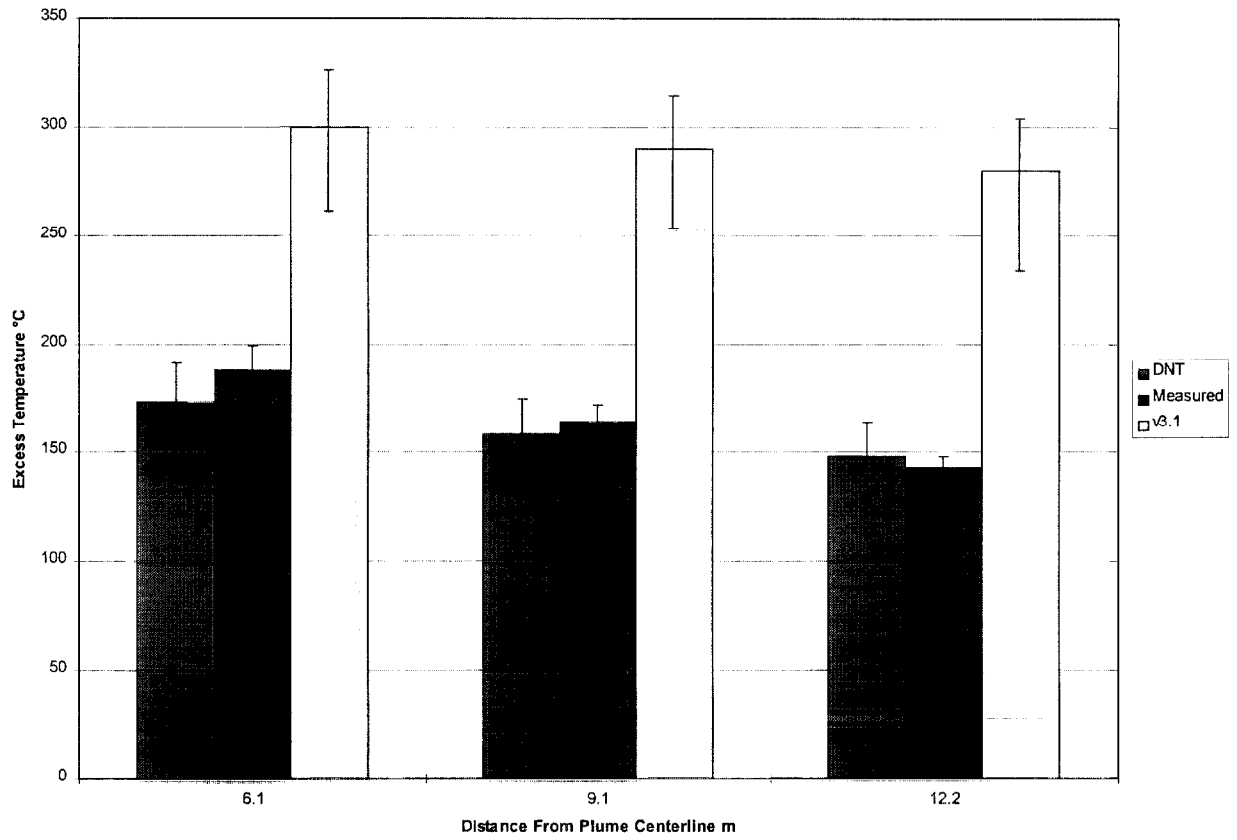


**Figure 19** Measured and predicted ceiling jet temperature excess for the 33 MW, 22 m experiment.

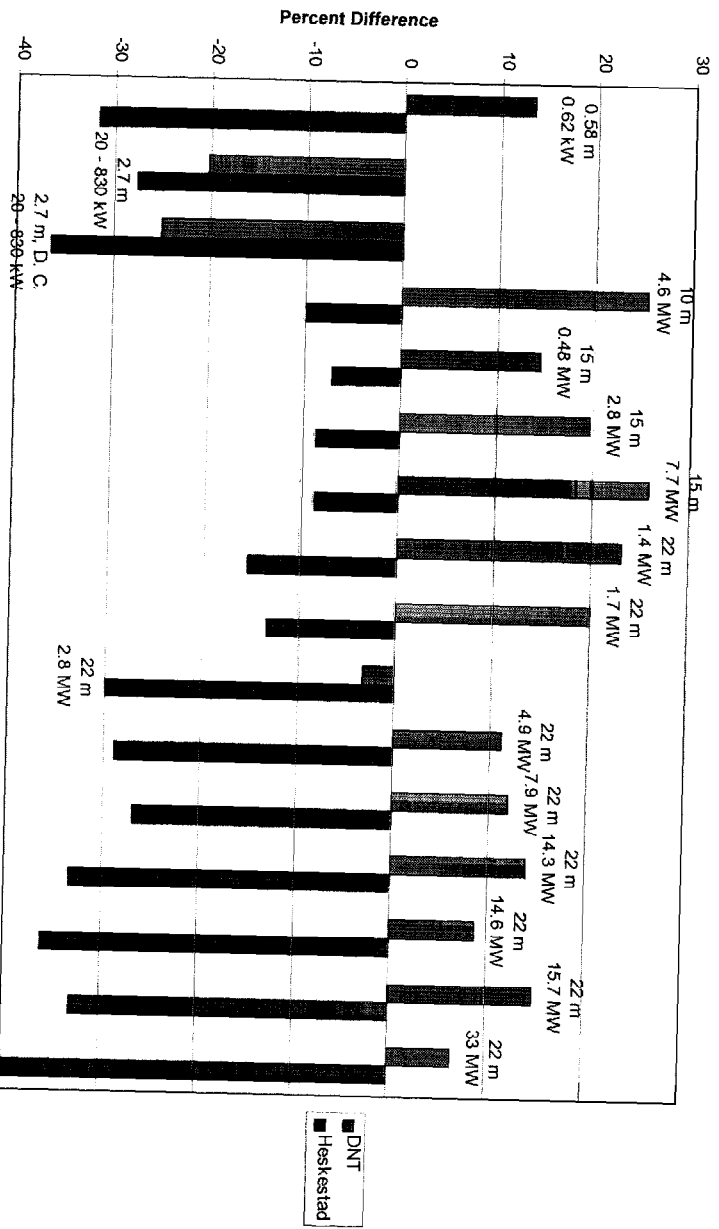


**Figure 20** Percentage difference, prediction minus measurement, for the plume centerline temperature excess for all experiments. For the 2.7 m experiments where comparisons were made based on a growing fire, the percentage difference is the average of all the comparisons.

### Ceiling jet Comparisons

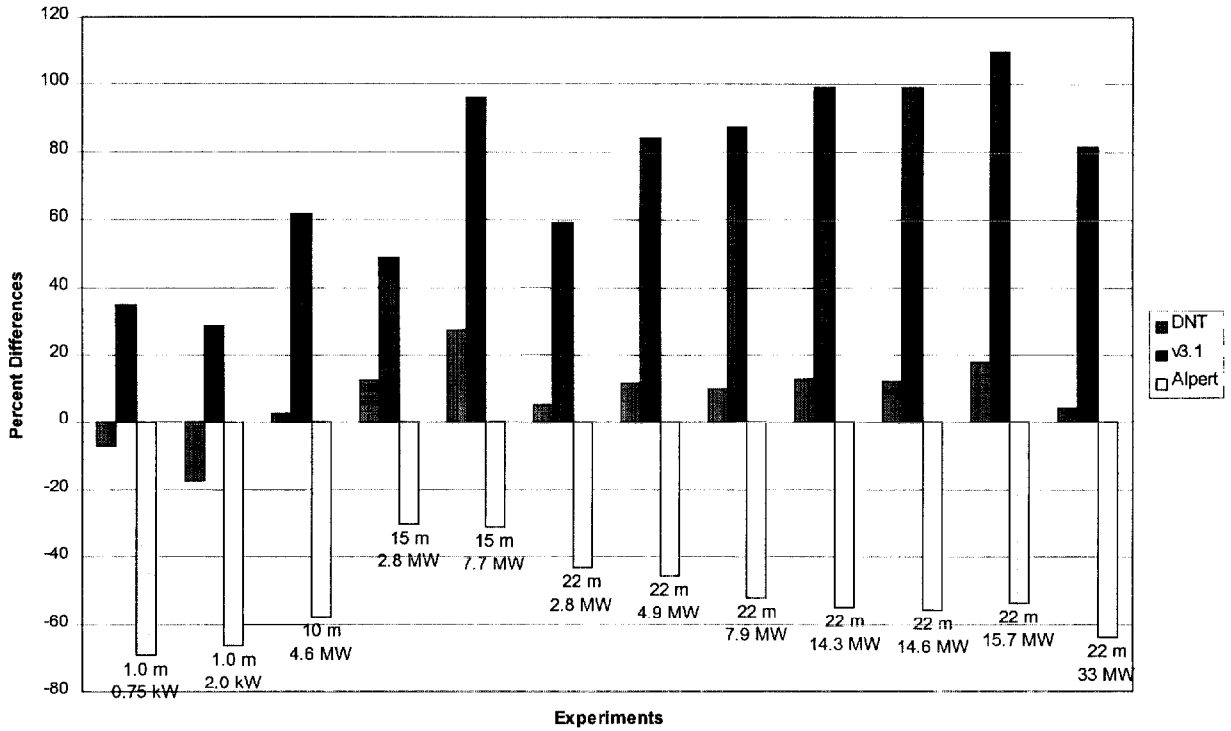


**Figure 21** Percentage difference, prediction minus experiment, for the ceiling jet temperature excess for all experiments. For each experiment, the percentage difference represents the average of the individual percent differences at each radial position.

|  |  |  |  |   |   |
|--|--|--|--|---|---|
| NIST-114<br>(REV. 6-93)<br>ADMAN 4.09  |  | <b>U.S. DEPARTMENT OF COMMERCE</b><br>NATIONAL INSTITUTE OF STANDARDS AND TECHNOLOGY |  | (ERB USE ONLY)  |   |
| <b>MANUSCRIPT REVIEW AND APPROVAL</b>  |  |  |  | ERB CONTROL NUMBER  | DIVISION<br>864                                   |
| INSTRUCTIONS: ATTACH ORIGINAL OF THIS FORM TO ONE (1) COPY OF MANUSCRIPT AND SEND TO THE SECRETARY, APPROPRIATE EDITORIAL REVIEW BOARD   |  |  |  | PUBLICATION REPORT NUMBER<br>NISTIR 6448  | CATEGORY CODE                                     |
|  |  |  |  | PUBLICATION DATE<br>January 2000  | NUMBER PRINTED PAGES                              |
| TITLE AND SUBTITLE (CITE IN FULL)  |  |  |  |   |   |
| Comparison of Algorithms to Calculate Plume Centerline Temperature and Ceiling Jet Temperature with Experiments  |  |  |  |   |   |
| CONTRACT OR GRANT NUMBER   |  |  | TYPE OF REPORT AND/OR PERIOD COVERED     |   |   |
| AUTHOR(S) (LAST NAME, FIRST INITIAL, SECOND INITIAL)<br>Davis, W. D  |  |  |  | PERFORMING ORGANIZATION (CHECK (X) ONE BOX)   |   |
|  |  |  |  | <input checked="" type="checkbox"/> NIST/GAITHERSBURG<br><input type="checkbox"/> NIST/BOULDER<br><input type="checkbox"/> JILA/BOULDER |   |
| LABORATORY AND DIVISION NAMES (FIRST NIST AUTHOR ONLY)<br>Building and Fire Research Laboratory, Fire Safety Engineering Division  |  |  |  |   |   |
| SPONSORING ORGANIZATION NAME AND COMPLETE ADDRESS (STREET, CITY, STATE, ZIP)   |  |  |  |   |   |
| PROPOSED FOR NIST PUBLICATION  |  |  |  |   |   |
| <input type="checkbox"/> JOURNAL OF RESEARCH (NIST JRES)   |  | <input type="checkbox"/> MONOGRAPH (NIST MN)   |  | <input type="checkbox"/> LETTER CIRCULAR  |   |
| <input type="checkbox"/> J. PHYS. & CHEM. REF. DATA (JPCRD)  |  | <input type="checkbox"/> NATL. STD. REF. DATA SERIES (NIST NSRDS)                    |  | <input type="checkbox"/> BUILDING SCIENCE SERIES  |   |
| <input type="checkbox"/> HANDBOOK (NIST HB)  |  | <input type="checkbox"/> FEDERAL INF. PROCESS. STDS. (NIST FIPS)                     |  | <input type="checkbox"/> PRODUCT STANDARDS  |   |
| <input type="checkbox"/> SPECIAL PUBLICATION (NIST SP)   |  | <input type="checkbox"/> LIST OF PUBLICATIONS (NIST LP)                              |  | <input type="checkbox"/> OTHER _____  |   |
| <input type="checkbox"/> TECHNICAL NOTE (NIST TN)  |  | <input checked="" type="checkbox"/> NIST INTERAGENCY/INTERNAL REPORT (NISTIR)        |  |   |   |
| PROPOSED FOR NON-NIST PUBLICATION (CITE FULLY)   |  |  | <input checked="" type="checkbox"/> U.S. | <input type="checkbox"/> FOREIGN  | PUBLISHING MEDIUM                                 |
|  |  |  |  |   | <input checked="" type="checkbox"/> PAPER         |
|  |  |  |  |   | <input type="checkbox"/> DISKETTE (SPECIFY) _____ |
|  |  |  |  |   | <input type="checkbox"/> OTHER (SPECIFY) _____    |
| SUPPLEMENTARY NOTES  |  |  |  |   |   |
| ABSTRACT (A 2000-CHARACTER OR LESS FACTUAL SUMMARY OF MOST SIGNIFICANT INFORMATION. IF DOCUMENT INCLUDES A SIGNIFICANT BIBLIOGRAPHY OR LITERATURE SURVEY, CITE IT HERE. SPELL OUT ACRONYMS ON FIRST REFERENCE.) (CONTINUE ON SEPARATE PAGE, IF NECESSARY.)   |  |  |  |   |   |
| <p>The predictive capability of algorithms designed to calculate plume centerline temperature and ceiling jet temperature in the presence of a hot upper layer using a two layer zone model approximation are compared with measurements from a series of experiments. The experiments included ceiling heights which ranged from 0.58 m to 22 m and heat release rates (HRR) from 0.62 kW to 33 MW. With the combined uncertainty of the measurement and the calculation roughly equal to plus or minus 20%, both algorithms consistently provided predictions either close to or within this uncertainty interval for all fire sizes and ceiling heights. Other algorithms included in the comparison are the ceiling jet algorithm of CFAST version 3.1, the unconfined plume algorithm of Heskestad, and the unconfined ceiling jet algorithm of Alpert.</p> |  |  |  |   |   |
| KEY WORDS (MAXIMUM OF 9; 28 CHARACTERS AND SPACES EACH; SEPARATE WITH SEMICOLONS; ALPHABETIC ORDER; CAPITALIZE ONLY PROPER)  |  |  |  |   |   |
| ceiling heights, ceiling jets, experiments, fire models, fire plumes, zone models  |  |  |  |   |   |
| AVAILABILITY   |  |  |  | NOTE TO AUTHOR(S): IF YOU DO NOT WISH THIS MANUSCRIPT ANNOUNCED BEFORE PUBLICATION, PLEASE CHECK HERE. <input type="checkbox"/>         |   |
| <input checked="" type="checkbox"/> UNLIMITED  |  | <input type="checkbox"/> FOR OFFICIAL DISTRIBUTION - DO NOT RELEASE TO NTIS          |  |   |   |
| <input type="checkbox"/> ORDER FROM SUPERINTENDENT OF DOCUMENTS, U.S. GPO, WASHINGTON, DC 20402  |  |  |  |   |   |
| <input checked="" type="checkbox"/> ORDER FROM NTIS, SPRINGFIELD, VA 22161   |  |  |  |   |   |

